16 QAM Modulation for High Capacity Digital Radio System

PHILIPPE DUPUIS, MICHEL JOINDOT, ALAIN LECLERT, AND DOMINIQUE SOUFFLET

Abstract—A computational method allowing the calculation of bit error rate in the presence of filtering and some other impairments is described for 16 QAM modulation; a breadboard working at a bit rate of 140 Mbits/s has been implemented and experimental results are compared with calculated values. The possible use of this modulation type for a high capacity digital radio-relay system is considered. Some parameters are introduced for this purpose, especially the net fade margin parameter. In the case of the 140 Mbit/s system in the 10.7-11.7 GHz frequency band, 4 PSK and 8 PSK modulation types are compared with 16 QAM. System gain, frequency arrangement, nodal capacity and outage performances are evaluated.

I—INTRODUCTION

THE development of high capacity digital radio relay systems leads to the use of high level modulation schemes: 8 PSK is currently used and 16 QAM (quadrature amplitude modulation) is now being investigated.

At first this paper presents the general features of 16 QAM modulation; a computer procedure which is briefly described allows the calculation of bit-error probability taking into account intersymbol interference and eventually some other impairments. In particular the influence of group delay and amplitude distortions was computed and the results were compared with measured values. Another computer simulation was carried on to take into account non-linear distortions—AM-AM and AM-PM conversion— and experimental and theoretical data are displayed.

After that, system parameters—in particular gross margin and net margin—are introduced to be used in the design of a radio link. They allow the computation probability of the outage when fading occurs.

These considerations are applied at a bit rate of 140 Mbits/s and in the 10.7-11.7 GHz frequency band which is assigned in France to digital systems [1]. Using the method which has been previously developed, the optimal frequency arrangement is determined for 4 PSK, 8 PSK and 16 QAM modulations. But it must be noted that these results can be extended to other bit rates and other frequency bands such as 6 GHz radio band.

A 16 QAM modem working at a bit rate of 140 Mbits/s and including a carrier recovery circuit (by the remodulation method) has been implemented in the CNET laboratories in Lannion. Experimental results (concerning the influence of filtering, distortions, sampling time errors, interferences) could

be obtained and compared with the computed values. One of these results is reported concerning group delay distortions.

II—16 QAM MODULATION

A—Description of the Modulation

16 QAM belongs to the general class of multiple amplitude and phase shift keying (MAPSK) modulations and the modulated signal can be represented by the following equation: [2]

$$U(t) = V \sum_k a_k X(t - kT) \cos \omega_0 t - b_k X(t - kT) \sin \omega_0 t. \tag{1}$$

ω_0 is related to the carrier frequency f_0 by the relation $\omega_0 = 2\pi f_0$, $X(t)$ is the elementary impulse shape defined by

$$X(t) = 1 \quad \text{if } t \in [0, T], X(t) = 0 \quad \text{if } t \notin [0, T] \tag{2}$$

V is a scaling factor.

We assume that a_k and b_k are two independent random variables which can take on four values $(-3, -1, 1, 3)$ with the same probability; furthermore we assume that a_k and a_l, b_k and b_l are independent $\forall k \neq l$.

Each value of a_k (resp. b_k) is associated with a state of the dibit $(A1, B1)$ (resp. $(A2, B2)$) where $A1, B1, A2, B2$ are binary data to be transmitted. We assume that the encoding rule is of the Gray type so that the two binary dibits associated with two consecutive values of a_k (resp. b_k) differ only by one bit.

The fig. 1 diagram shows the sixteen amplitude and phase levels of the modulated signal $u(t)$ with the corresponding four bit words $(A1, B1, A2, B2)$.

Communication theory gives the structure of the optimal receiver and the error probability when the signal is observed in the presence of an additive white Gaussian noise (AWGN) with two-sided spectral density $N_0/2$ which represents quite well the thermal noise of the radio link receiver. Figure 2 shows the scheme of the optimum receiver. M.F. is the matched filter with impulse response $X(t)$. It is followed by a sampler and a threshold circuit for the decision. As we are primarily interested in the error probability on each of the data streams $A1, B1, A2, B2$, we will express the error probability P_e^{Ai} (resp. P_e^{Bi}) defined by:

$$P_e^{Ai} = P(\hat{A}_i \neq A_i) \quad P_e^{Bi} = P(\hat{B}_i \neq B_i) \tag{3}$$

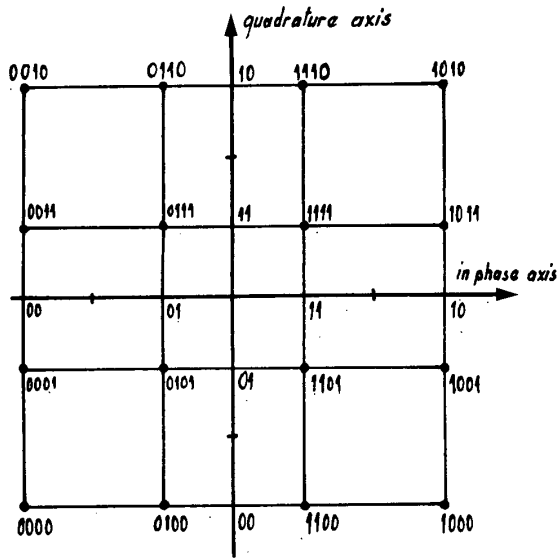where A_i is the output of the decision circuit.

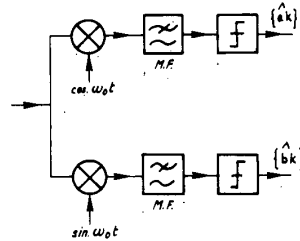FIG. 1   Constellation of the 16 QAM modulation

FIG. 2   Optimum receiver for 16 QAM signal

At the output of the matched filter, the signal can take on four values at the sampling time: $\pm VT$, $\pm 3VT$. The noise is Gaussian and its variance is $\sigma_0{}^2 = N_0 T^{-1}$. With the assumption that $V^2 T N_0{}^{-1}$ is sufficiently large—and it is valid in our case—the bit error probability can be expressed by the following relationship:

$$P_e{}^{A1} = P_e{}^{A2} = \tfrac{1}{2} P_e{}^{B1} = \tfrac{1}{2} P_e{}^{B2} = \tfrac{1}{4}\,\mathrm{erfc}\left(\frac{V^2 T}{2N_0}\right)^{1/2} \quad (4)$$

erfc X is the complementary error function defined by the following formula

$$\mathrm{erfc}\,X = \frac{2}{\sqrt{\pi}} \int_X^{+\infty} \exp - t^2\, dt. \quad (5)$$

$V^2 T(2N_0)^{-1}$ can be regarded as the ratio of $V^2/2$ to the noise power contained in the Nyquist frequency band $[f_0 - (2T)^{-1}, f_0 + (2T)^{-1}]$. Starting from (4) we can write two slightly different expressions of $P_e{}^{Ai}$.
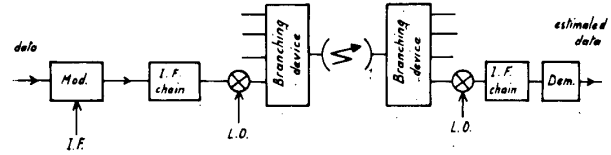

FIG. 3   Simplified scheme of the radio link

Introducing the average power P_m and the peak power P_c of the signal $u(t)$ we can write:

$$P_e{}^{A1} = P_e{}^{A2} = \tfrac{1}{4}\,\mathrm{erfc}\left(\frac{P_m}{10\sigma_0{}^2}\right)^{1/2} = \tfrac{1}{4}\,\mathrm{erfc}\left(\frac{Pc}{18\sigma_0{}^2}\right)^{1/2}. \quad (6)$$

As "signal to noise" ratios are usually expressed in dB we will introduce CNR_0 defined as:

$$\mathrm{CNR}_0 = 10 \log_{10} \frac{P_m}{\sigma_0{}^2}. \quad (7)$$

CNR_0 is the ratio (expressed in decibel) of the average power of the carrier to the noise power contained in the Nyquist bandwidth. The error probability can be plotted versus CNR_0: the curve obtained in these conditions will be referred to as "theoretical curve" in further computations and used as a reference in the presence of impairments. The excess amount of CNR_0 to be provided will be called "CNR_0 degradation". It depends obviously on the error probability.

B–Transmission of 16 QAM Modulation of a Radio-Link Channel

The transmission channel including transmitting and receiving equipments can be represented by figure 3.

Besides the unavoidable degradation due to filtering, other transmission impairments occur, mainly due to:

—thermal noise appearing in the resistive parts of the receiving chain
—radio-frequency interference
—various imperfections (decision threshold shifts, error on sampling time).

All these impairments are listed in table 1. At first, non linear distortions will not be taken into account.

The system of figure 3 can be represented by using the low-pass equivalent channel as shown in Figure 4. Let us define the complex envelope $U(t)$ by the relationship:

$$u(t) = \mathrm{Re}\,[U(t)\exp i\omega_0 t]. \quad (8)$$

(8) gives immediately:

$$U(t) = V \sum_k (a_k + ib_k)X(t - kT)$$

$$= V \sum_k c_k X(t - kT) \sum_k c_k X(t - kT). \quad (9)$$

TABLE 1

Impairment (error rate : 10^{-4})		Equivalent degradation	
		CNR	eye-aperture
Filtering (Butterworth 5th order)	RF.TX 1.2S RF.RX 2.0S IF.RX 1.2S	1.6 dB	16 %
Residual distortion Group-delay 0.7 ns Amplitude 0.6 dB		0.2 dB 0.6 dB	2 % 5,5 %
Phase errors Modulator 1° Demodulator 2°		0.7 dB	7 %
Regenerator : decision level drift 0.5 dB		0.3 dB	3 %
Timing phase error $\frac{1}{40\ s}$		0.3 dB	3 %
TWT non-linearities :8dB Backoff (average power)		1 dB	10 %
Local interference carrier CIR = 30 dB		0.2 dB	2 %
Overall eye-aperture degradation			48,5 %
Overall CNR degradation		5.5. dB	

Now we use the very classical result: if $v(t)$ is the response of a linear filter (complex gain $G(f)$) to the input signal $u(t)$, then the complex envelope $V(t)$ of $v(t)$ is the response of the so-called low-pass equivalent filter (complex gain $G_0(f)$) to the complex envelope $U(t)$ of $u(t)$.

$H_T(f)$ is the transfer function of a filter which is the low-pass equivalent of the cascade of I.F. transmitting filters, branching filters, and eventually other linear filtering effects like selective fading. $H_R(f)$ is the transfer function of the low-pass equivalent of the I.F. receiving filter, and baseband filters before decision.

The noise is a complex white Gaussian one. The complex decision device—complex representation of the demodulation—determines $\hat{c}_k$ (that is to say $\hat{a}_k$ and $\hat{b}_k$) as a function of the region where the observation is located.

The observation at the input of the decision device, at the sampling time t_e, can be written:

$$Z(t_e) = V \sum_k c_k[P(t_e - kT) + iQ(t_e - kT)]$$
$$+ n_c(te) + in_s(te). \qquad (10)$$

$P(t) + iQ(t)$ is the response of the global transmission filter (complex gain $H_T(f) \cdot H_R(f)$) to the fundamental impulse $X(t) \cdot n_c(t_e)$ and $n_s(t_e)$ are Gaussian random variables uncorrelated, with a variance σ^2:

$$\sigma^2 = N \int_{-\infty}^{\infty} |H_R(f)|^2\, df = N_0 B_R. \qquad (11)$$
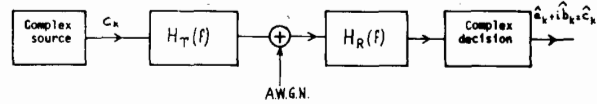

FIG. 4   Low-pass equivalent model of the transmission system

B_R is the noise-bandwidth of the receiving filter.

By dividing $Z(t_e)$ in its real and imaginary parts X and Y, writing P_k, Q_k, n_c, n_s instead of $P(t_e - kT)$, $Q(t_e - kT)$, $n_c(t_e)$, $n_s(t_e)$ and considering the decision relative to a_0 and b_0 (this choice is unrestrictive because of stationarity) (10) becomes:

$$X = V \left[a_0 P_0 - b_0 Q_0 + \sum_{k \neq 0} (a_k P_k - b_k Q_k) \right] + n_c$$

$$Y = V \left[b_0 P_0 + a_0 Q_0 + \sum_{k \neq 0} (b_k P_k + a_k Q_k) \right] + n_s. \qquad (12)$$

(12) can be rewritten in a more condensed form by introducing the random variables z_c and z_s defined by:

$$z_c = - b_0 Q_0 + \sum_{k \neq 0} (a_k P_k - b_k Q_k),$$

$$z_s = a_0 Q_0 + \sum_{k \neq 0} (b_k P_k + a_k Q_k). \qquad (13)$$

If we assume that the decision boundaries for X and Y observations are defined by X (resp. Y) equal to 0 or $\pm 2 P_0 V$, if we assume furthermore that the ratio $P_0 V \sigma^{-1}$ is sufficiently large so that the probability of overcrossing more than one decision boundary can be neglected, then the bit error probabilities defined by (3) can be expressed in the following form:

$$P_e{}^{A1} \mid z_c = \tfrac{1}{4} P\left(\mid z_c + \frac{n_c}{V} \mid > P_0 \right) = \tfrac{1}{2} P_e{}^{B1} \mid z_c \qquad (14a)$$

$$P_e{}^{A2} \mid z_s = \tfrac{1}{4} P\left(\mid z_s + \frac{n_s}{V} \mid > P_0 \right) = \tfrac{1}{2} P_e{}^{B2} \mid z_s \qquad (14b)$$

where $P_e \mid z$ is the error probability conditionally to some given value of a random variable z.

(14a) and (14b) can be simplified by using the assumption about "a priori" distributions of a_k and b_k; then z_c and z_s have the same probability density function which is even. As the Gaussian law of n_c and n_s is also even, then the following relation holds:

$$P_e{}^{A1} = P_e{}^{A2} = \tfrac{1}{2} P_e{}^{B1} = \tfrac{1}{2} P_e{}^{B2}$$

$$= E_z \left[\tfrac{1}{4} \, \text{erfc} \, \frac{V(P_0 + z)}{\sigma\sqrt{2}} \right]. \qquad (15)$$

z is a random variable defined by

$$z = a_0 Q_0 + \sum_{k \neq 0} b_k P_k + a_k Q_k \tag{16}$$

where a_k and b_k are discrete random variables satisfying the "a priori" conditions defined in the beginning.

The exact calculation of (15) is difficult: when P_k and Q_k are non-zero terms only if k belongs to a finite set, z is a discrete random variable and (15) can be performed by the so-called exhaustive method. Even in this case however, a large amount of computer time is required.

It is the reason why we preferred to use a Gram Charlier expansion of (15) given by Ho and Yeh [2]. This method requires only the knowledge of the moments of the random variable z. Since z is even, only the even-order moments M_{2k} are non-zero and (15) can be written:

$$P_e{}^{A1} = \tfrac{1}{2} \operatorname{erfc} \frac{P_0 V}{\sigma \sqrt{2}} + \frac{1}{\sqrt{\pi}}$$

$$\cdot \exp - \frac{P_0{}^2 V^2}{2\sigma^2} \sum_{k=1}^{+\infty} \frac{M_{2k}}{(2k)!(2\sigma^2)^k} H_{2k-1}\left(\frac{P_0 V}{\sigma \sqrt{2}}\right). \tag{17}$$

$H_n(x)$ is the nth order Hermite polynominal.

It can be shown [3] that this series is absolutely convergent.

Only a finite number of terms must be kept for the practical computational procedure.

The error probability given by (15) can be plotted versus $\mathrm{CNR_0}$; but it is also convenient to introduce a slightly different parameter called CNR defined by the formula:

$$\mathrm{CNR} = 10 \log_{10} \frac{P_m}{\sigma^2}. \tag{18}$$

The following relation between CNR and $\mathrm{CNR_0}$ holds:

$$\mathrm{CNR} = \mathrm{CNR_0} - 10 \log_{10} B_R T. \tag{19}$$

The $\mathrm{CNR_0}$ and CNR degradations in the presence of an impairment will be respectively referred as $\mathrm{DCNR_0}$ and DCNR.

It is interesting to note that if we consider a filter satisfying Nyquist's criteria shaped by the Fourier transform of $X(t)$, z becomes identically 0 and (15) becomes:

$$P_e{}^{A1} = P_e{}^{A2} = \tfrac{1}{2} P_e{}^{B1} = \tfrac{1}{2} P_e{}^{B2} = \tfrac{1}{4} \operatorname{erfc} \frac{V}{\sigma \sqrt{2}}$$

$$= \tfrac{1}{4} \operatorname{erfc} \left(\frac{P_m}{\sigma^2}\right)^{1/2}. \tag{20}$$

The curve giving $P_e{}^{A1}$ versus CNR with Nyquist's filtering is the same as with the optimum receiver; but the two curves versus $\mathrm{CNR_0}$ are not identical because the noise bandwidth of shaped Nyquist's filter exceeds the Nyquist's bandwidth.

C–Description of the Computational Procedure and Examples of Application

P_k and Q_k are obtained by a Fast Fourier Transform from the frequency domain transfer function $H_T(f) \cdot H_R(f)$. In most of the examples the filters were of Butterworth type with 3, 4 or 5 poles; but obviously any other choice remains possible and numerical values of amplitude and group-delay obtained from measurements could be introduced.

The moments of z are obtained in reference [3] by a recurrence formula; unfortunately we found that in some cases when the intersymbol interference became too large, the method could not be used because some moments were negative. So we had to use a classical method which requires much more time than the recurrence computation.

$$M_{2k} = \sum_i z_i{}^{2k} P(z = z_i). \tag{21}$$

The sum is taken over all the possible values of the random variable z which is discretized by truncation of (16). Obviously in the case of "Hermitian symmetry" a lot of time can be saved because Q_k is identically zero. This situation was encountered in many numerical applications with Butterworth filters. The number of terms kept after truncation of (16) can be chosen versus the impulse response of the channel, carrier to noise ratio, and required accuracy.

At first we looked at the influence of a single I.F. filter, $H_T(f)$ being assumed to be equal to unity. The $\mathrm{DCNR_0}$ and DCNR degradations at $P_e = 10^{-5}$ are plotted on fig. 5 versus the reduced 3 dB bandwidth, BT, of the I.F. filter (5th order perfectly group delay equalized Butterworth filter). This type of I.F. filter will be kept in the following example. A perfectly group delay equalized Butterworth filter will be referred further as a PEB filter.

Some other computations, detailed in [4], were performed for different radio-frequency filtering arrangements. For instance, figure 6 represents $\mathrm{DCNR_0}$ versus BT (defined in the same manner as in fig. 5) for four filtering arrangements. $H_T(f)$ is obtained by cascading two 5th order PEB filters, a receiving one with reduced bandwidth 2, and a transmitting one with various reduced bandwidths $B_t T$.

The influence of various group-delay or amplitude distortions resulting from non perfect equalization was also investigated [3] using the computer procedure which has been just described.

As an example, let us assume a linear group-delay distortion in the filtering conditions of figure 6 with $B_t T = 2$ and $BT = 1.15$ (40 MHz for 140 Mbit/s bit rate). Measured and computed $\mathrm{DCNR_0}$ (respectively dotted and solid line) are plotted on figure 7 versus peak to peak group delay distortion in 40 MHz bandwidth.

Let us now consider the influence of interferences which is of primary importance in the analysis and design of a radio link. All the interferers will be assumed to be sinusoidal.

The error probability can now be expressed by the relationship

$$P_e{}^{A1} = E_{z_1}\left[\tfrac{1}{4} \operatorname{erfc} \frac{V(P_0 + z_1)}{\sigma \sqrt{2}} \right]. \tag{22}$$
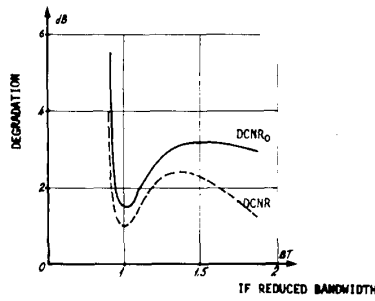
FIG. 5   Degradation of CNR_0 and CNR versus reduced bandwidth of the receiving IF filter
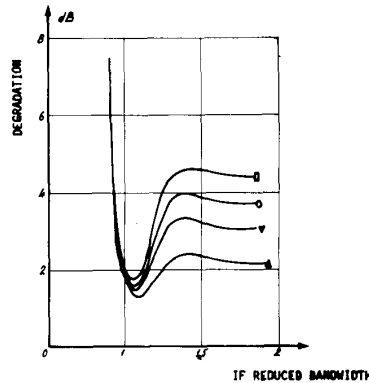

FIG. 6   Degradation of CNR_0 versus bandwidth of the IF receiving filter for different transmitting filter reduced bandwidths: □ 1.4; ○ 1.6; ▽ 1.8; △ 2.0.
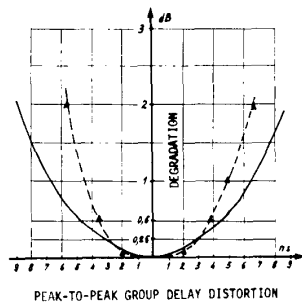

FIG. 7   Degradation of CNR_0 with linear group-delay distortion versus peak to peak value in 40 MHz (bit rate: 140 Mbits/s−IF bandwidth− B = 40 MHz); solid line−calculated curve; dashed line−experimental results.

z_1 appears as the sum of z (previously defined) and of the low-pass equivalent of the interferers taken at the sampling time. A new parameter called CIR (carrier to interference ratio) is defined by the formula:

$$CIR = 10 \log_{10} \frac{P_m}{P_I} . \tag{23}$$
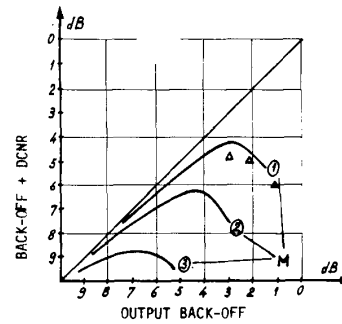
P_I is the r.m.s. power of the interference.

FIG. 8   Degradation due to TWT amplifier non-linearities; solid line: calculated, △: experimental data. *Note:* M hop configuration includes $(M - 1)$ heterodyne repetitions.

It is now clear that the computation procedure can be generalized without any more difficulty if we can compute the moments of the new random variable z_1. The computation is particularly simple with only one interferer and no inter-symbol interference (optimum receiver or Nyquist's filtering). Then it can be shown classically that the same $DCNR_0$ is obtained with 16 QAM modulation for some CIR and with BPSK for CIR + 10 dB.

In order to take into account the impairments due to non linearities, a computer simulation program has been used. The non linear amplifier is modeled by its AM-AM non linearity and AM-PM conversion. Plotted on fig. 8 is the sum of the power back-off and the degradation of CNR due to the amplifier versus the back-off. Experimental data are also given. Curves corresponding to an amplification without regeneration over two or three hops are displayed.

III−PARAMETERS USED FOR THE DESIGN OF A DIGITAL RADIO SYSTEM

A−Equipments

CNR_a and CNR_b

For any modulation scheme, as for 16 QAM modulation, a theoretical curve can be computed. If an error rate value is specified, a value of CNR_0 is then specified too. Because of the various impairments the CNR required to obtain the specified error-rate is CNR_0 plus some degradation DCNR. This degradation can be evaluated by an equivalent eye aperture method [5]:

$$DCNR = -20 \log_{10} \left(1 - \sum E_{eq}\right) \tag{24}$$

where E_{eq} is the equivalent eye aperture degradation (percent of the total aperture) due to one impairment.

For example table 1 gives the degradation allocation for the 16 QAM modem implemented in our laboratory.

The practical carrier to noise ratio CNR corresponding to the outage error rate (e.g. 10^{-4}) is referred to as $CNR_a \cdot CNR_b$ is related to the error rate (e.g. 10^{-10}) during nominal unfaded signal conditions. Table 2 gives the values of CNR_a and CNR_b for three modulations.

The third parameter is the adjacent channel interference reduction factor (IRF) obtained from filtering. It is the ratio

DOCKET ALARM

Explore Litigation Insights

Docket Alarm provides insights to develop a more informed litigation strategy and the peace of mind of knowing you're on top of things.

Real-Time Litigation Alerts

Keep your litigation team up-to-date with **real-time alerts** and advanced team management tools built for the enterprise, all while greatly reducing PACER spend.

Our comprehensive service means we can handle Federal, State, and Administrative courts across the country.

Advanced Docket Research

With over 230 million records, Docket Alarm's cloud-native docket research platform finds what other services can't. Coverage includes Federal, State, plus PTAB, TTAB, ITC and NLRB decisions, all in one place.

Identify arguments that have been successful in the past with full text, pinpoint searching. Link to case law cited within any court document via Fastcase.

Analytics At Your Fingertips

Learn what happened the last time a particular judge, opposing counsel or company faced cases similar to yours.

Advanced out-of-the-box PTAB and TTAB analytics are always at your fingertips.

API

Docket Alarm offers a powerful API (application programming interface) to developers that want to integrate case filings into their apps.

LAW FIRMS

Build custom dashboards for your attorneys and clients with live data direct from the court.

Automate many repetitive legal tasks like conflict checks, document management, and marketing.

FINANCIAL INSTITUTIONS

Litigation and bankruptcy checks for companies and debtors.

E-DISCOVERY AND LEGAL VENDORS

Sync your system to PACER to automate legal marketing.

fastcase
Smarter legal research.